Defect structure of a nematic liquid crystal around a spherical particle: Adaptive mesh refinement approach

Jun-ichi Fukuda,[1] Makoto Yoneya,[1] and Hiroshi Yokoyama[1,2]
[1]*Yokoyama Nano-Structured Liquid Crystal Project, ERATO, Japan Science and Technology Corporation, 5-9-9 Tokodai, Tsukuba 300-2635, Japan*
[2]*Nanotechnology Research Institute, AIST, 1-1-4 Umezono, Tsukuba 305-8568, Japan*
(Received 11 April 2001; published 4 April 2002)

We investigate numerically the structure of topological defects close to a spherical particle immersed in a uniformly aligned nematic liquid crystal. To this end we have implemented an adaptive mesh refinement scheme in an axi-symmetric three-dimensional system, which makes it feasible to take into account properly the large length scale difference between the particle and the topological defects. The adaptive mesh refinement scheme proves to be quite efficient and useful in the investigation of not only the macroscopic properties such as the defect position but also the fine structure of defects. It can be shown that a hyperbolic hedgehog that accompanies a particle with strong homeotropic anchoring takes the structure of a ring.

DOI: 10.1103/PhysRevE.65.041709 PACS number(s): 61.30.Cz, 61.30.Jf, 82.20.Wt

Topological defects [1–3] are associated with broken continuous symmetry and can be found in various condensed matter systems. They have attracted great interests in the viewpoint of physics as well as mathematics because the macroscopic properties are often influenced by the presence of topological defects. Among such systems showing topological defects, liquid crystals [4,5] have proven to be one of the best examples for the investigation of the properties of topological defects, because they are easily accessible and controlled experimentally and show a rich variety of qualitatively different defects.

Recently, a new class of liquid crystal emulsions and colloids, isotropic liquid droplets or solid macroparticles dispersed in a nematic host fluid, has been reported [6–9] to show that depending on the properties of surface anchoring, a rich and nontrivial variety of topological defects, such as a hyperbolic hedgehog [6,7], an equatorial Saturn ring [8,9] and boojums [7] appear close to the droplets or macroparticles. In particular, the formation of a hyperbolic hedgehog is not trivial as compared with a Saturn ring that was focused on in earlier theoretical work [10,11], and several theoretical [12,13] and numerical [14–16] studies have been devoted to the understanding of the properties of a hyperbolic hedgehog. One of the interesting results obtained by numerical analyses is that the equilibrium configuration of the topological defect accompanying a particle with strong homeotropic surface anchoring depends on the ratio between the defect core radius r_c and the radius of the particle R_0. A hyperbolic hedgehog is stable when the defect size is small enough, i.e., $r_c/R_0 \lesssim 0.05$, while a Saturn ring is preferred for $r_c/R_0 \gtrsim 0.05$ [15]. However, in the previous numerical studies based on a continuum description [14,15], the topological defect was treated as a singular point and the defect core region was considered indirectly by introducing a core energy separately and a cutoff around the singularities. This is because the direct and precise numerical treatment encounters a serious problem associated with a high resolution required for the description of the defect core region. To obtain direct evidence of the transition between a hyperbolic hedgehog and a Saturn ring numerically, we have to treat a defect smaller than $0.05R_0$, which requires a numerical lattice whose grid spacing is $10^{-2}R_0$ or smaller. Moreover, since the defect size r_c is of the order 10 nm and the typical droplet radius R_0 in the experiments is larger than 1 μm [6–9], in realistic situation we have $r_c/R_0 \lesssim 10^{-2}$. Such a large scale difference should be problematic also in molecular dynamics simulations [16,17], because a huge number of molecules must be necessary to reproduce a system with $r_c/R_0 \ll 1$. Therefore, the presence of these two characteristic lengths r_c and R_0 with large scale difference makes it quite difficult and challenging to investigate directly the structure and the properties of topological defects by numerical simulations.

One of the possible ways to overcome the numerical difficulty arising from the limit of numerical resources and the requirement of a fine resolution is to use an adaptive mesh refinement (AMR) technique [18], where finer numerical grids are dynamically generated only in the regions of interest with a strong variation of the spatial structures. In our previous study [19], we adopted this AMR scheme and showed its usefulness for the investigation of topological defects in liquid crystals for the first time. Although our treatment was restricted to two-dimensional cases, the minimum grid size could be taken smaller than $10^{-3}R_0$ within an acceptable numerical cost, which gives a resolution fine enough to simulate the defect core, whose radius is of the order $10^{-2}R_0$. In this paper we extend our previous numerical implementation to an axi-symmetric three-dimensional case to investigate directly the effect of the defect size on the equilibrium configuration of the topological defect in a nematic liquid crystal around a spherical particle.

To describe the orientational profile of nematic liquid crystals we adopt the traceless tensor order parameter of second rank Q_{ij} instead of the director $\boldsymbol{n}$ that most of the previous numerical studies, using a continuum description [14,15], employed. In the tensor description, topological defects do not appear as singularities and we do not have to deal with them separately. We consider the case where a spherical particle of radius R_0 with the strong homeotropic

anchoring on the surface is immersed in a uniformly aligned nematic liquid crystal. In the strong anchoring limit, the anchoring can be taken into account as the boundary condition at $r=R_0$, $Q_{ij}=Q_s(e_{ri}e_{rj}-1/3\delta_{ij})$, where the center of the spherical particle is located at the origin and $\boldsymbol{e}_r$ is the unit vector in the radial direction. The degree of orientational order at the surface Q_s will be taken to be equal to that of the bulk Q_b. The free energy of the system can be written as

$$F=\int_{r>R_0} d\boldsymbol{r}\left[\left(-\frac{1}{2}A\,\mathrm{Tr}\,\mathsf{Q}^2+\frac{1}{3}B\,\mathrm{Tr}\,\mathsf{Q}^3+\frac{1}{4}C(\mathrm{Tr}\,\mathsf{Q}^2)^2\right)+\frac{1}{2}L_1\partial_k Q_{ij}\partial_k Q_{ij}-\lambda\,\mathrm{Tr}\,\mathsf{Q}\right], \tag{1}$$

where the first three terms are the bulk energy in terms of the Landau–de Gennes expansion with $\mathrm{Tr}\,\mathsf{Q}^2=Q_{ij}Q_{ji}$ and $\mathrm{Tr}\,\mathsf{Q}^3=Q_{ij}Q_{jk}Q_{ki}$ (hereafter summations over repeated indices are implied). The coefficient C must be positive and the isotropic state $Q_{ij}=0$ becomes unstable to form an ordered phase when $A>0$. The coefficients in the simulations are chosen as $C=-B=3A$ so that the uniaxial configuration $Q_{ij}=Q_b(n_in_j-1/3\delta_{ij})$ with $Q_b=1$ minimizes the bulk energy. Although this is not a unique choice for the coefficients of the bulk energy, we believe that the difference of the coefficients affects only the fine, possibly biaxial, structure of the defect core [20]. We adopt the simple one-constant form with the elastic constant L_1 as the elastic energy. The last term with the Lagrange multiplier λ is added to ensure $\mathrm{Tr}\,\mathsf{Q}=Q_{ii}0$. So long as the equilibrium configuration is concerned, the unique relevant dimensionless parameter is the ratio of the two characteristic lengths, the nematic coherence length $\sqrt{L_1/A}$ and the particle radius R_0. We will denote it by $\xi\equiv\sqrt{L_1/A}/R_0$.

We restrict ourselves to an axi-symmetric case and the complex defect structure as reported by Gu and Abbott [9] is beyond the scope of our study. We take the z axis as the symmetry axis, which is parallel to the orientation of the liquid crystal far away from the spherical particle. The orientational order at (r,θ,φ) in the polar coordinate is then written as $Q_{ij}(r,\theta,\varphi)=R_{ik}(\varphi)R_{jl}(\varphi)Q_{kl}(r,\theta,\varphi=0)$, where $R(\varphi)$ is the operator of rotation around the z axis by the angle φ, and summations over k and l are implied. Therefore, the treatment of the order parameter at $\varphi=0$ is sufficient and the problem is reduced to a two-dimensional one.

In our numerical system we first make a transformation $\zeta=R_0^{-1}-r^{-1}$ and prepare in the (ζ,θ) space a $L_\zeta\times L_\theta=32\times64$ rectangular lattice with equal grid spacings. The advantage of introducing ζ is that the infinite space with $r\geqslant R_0$ is mapped to the finite region $\zeta=[0,R_0^{-1}]$. Moreover, even without the mesh refinement, the grid size in the real space is smaller when the grids are closer to the surface of the particle, where strong variation of the orientational order is expected. Our adaptive mesh scheme here is similar to those originally introduced in Ref. [18] and utilized in our previous study [19]. We allow mesh refinement up to eight levels and our numerical system, thus, corresponds to $2^{13}\times2^{14}$ nonadaptive grids. The finest grid size in real space is then approximately $(1.2\times10^{-4}R_0)\times(1.9\times10^{-4}R_0)$.

In this study we concentrate our attention to the hedgehog configuration and the corresponding equilibrium profile is obtained by relaxing the system through the dynamics of model A [21]: $\partial Q_{ij}/\partial t=-\delta F/\delta Q_{ij}$, where the time t has been rescaled so that the kinetic coefficient is equal to unity. We first perform a simulation with $\xi^2=(8/3)\times10^{-4}$ ($\xi=1.633\times10^{-2}$) under the initial configuration prepared by spinning around the symmetry axis the exact orientation profile in two dimensions [4,12,19] with two $-1/2$ defects located at $(r,\theta)=(1.2,\pm2°)$. To reduce the numerical time to achieve the equilibrium state, simulations for all the other ξ's are carried out using the equilibrium profile of $\xi=1.633\times10^{-2}$ as the initial condition.

In Fig. 1 we show the equilibrium orientation profile of a hedgehog configuration and the corresponding numerical grids for $\xi=2\times10^{-3}$. Although it is not apparent in Fig. 1(a), the magnified plot of $\mathrm{Tr}\,\mathsf{Q}^2$ in Fig. 1(b) obviously reveals that the accompanying topological defect is a ring, not a point as believed in previous experimental [6,7] and theoretical [12–15] studies. We have checked that even when we use an orientation profile with one point defect as the initial condition, the point defect relaxes to form a ring. Therefore, the formation of a ring is not an artifact arising from the choice of the initial condition. To check quantitatively the effect of the variation of ξ [22] on the ring defect configuration, we plot in Fig. 2 the radius of the disclination ring as a function of ξ. We note that for $\xi\gtrsim1.8\times10^{-2}$, the hedgehog configuration becomes unstable to form an equatorial Saturn ring. When ξ is small enough, the ring radius R_{ring} satisfies $R_{ring}/R_0\simeq5.5\xi$. This implies that the ring is not seriously disturbed by the particle when R_{ring} is small. In other words, when the particle radius R_0 is large enough compared to the size of the defect, the nematic coherence length (ξR_0 in a dimensional form) is the unique length scale that determines the spatial structure of the topological defect and the defect ring radius R_{ring} is, thus, proportional to ξR_0, i.e., $R_{ring}/R_0\propto\xi$. For large ξ, R_{ring}/R_0 deviates to a larger value from 5.5ξ, which indicates that the radial director configuration around the particle tends to open the disclination ring further. We note that the ringlike hedgehog may be a metastable state, in particular for large ξ. The comparison of the free energy between the hedgehog and the Saturn ring is necessary to determine whether the hedgehog configuration is really stable and will be given in a future paper.

The distance of the center of the ring r_d from the center of the particle is also plotted in Fig. 3. For $\xi\lesssim10^{-2}$, r_d/R_0 is almost independent of ξ and lies in the range $1.2405<r_d/R_0<1.2425$, close to the values obtained in previous studies [12,14,15]. The ring defect lies closer to the particle when $\xi\gtrsim10^{-2}$ and ξ (and correspondingly, the radius of the ring) becomes larger. This is in agreement with an intuitive argument that the repulsion between the defect and the particle induced by the elastic deformation of the director field should be weaker when the ring becomes larger and the director field can relax to produce weaker elastic deformation.

We note here that it was concluded in Ref. [12] that a hyperbolic disclination ring is unstable to shrink to a point, in contrast to our numerical study. Their argument is based on a rough estimate of the ring radius, which gives

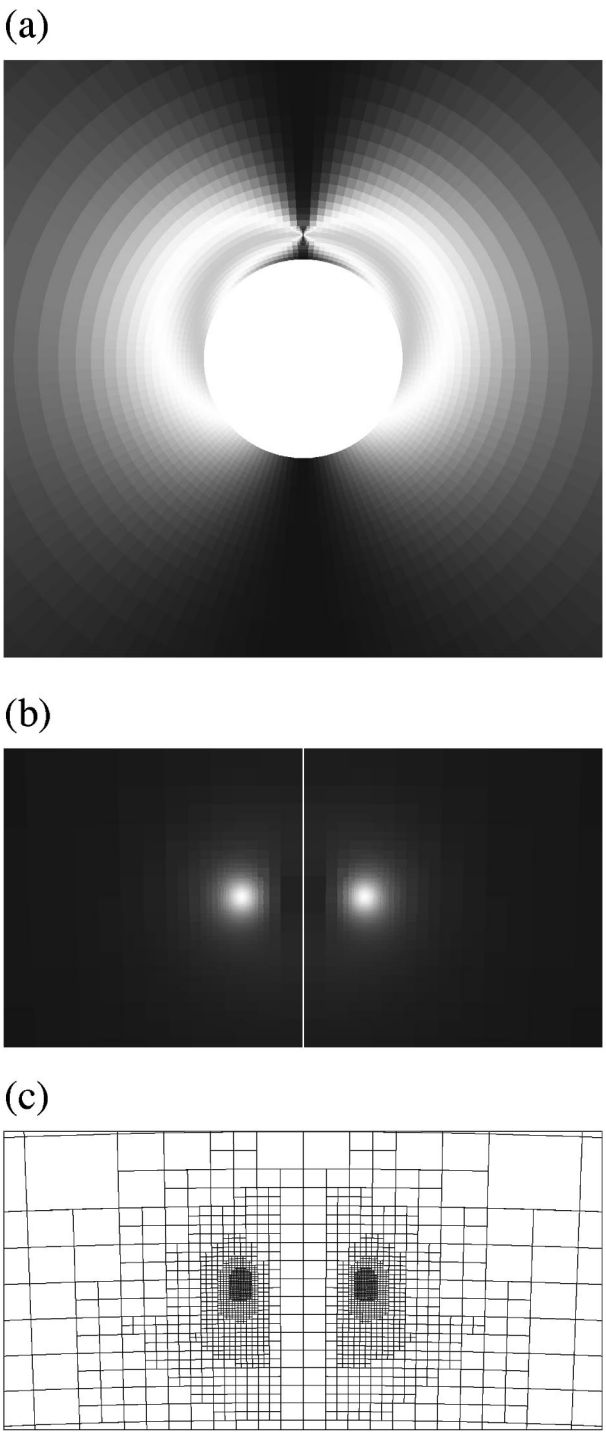

FIG. 1. (a) The orientation profile for $\xi=2\times10^{-3}$. The darkness is proportional to Q_{zz}^2. The symmetry axis, or the z axis is along the vertical direction. (b) The grayscale plot of the degree of orientational order $\mathrm{Tr}\,\mathbf{Q}^2$. The whiter region indicates smaller $\mathrm{Tr}\,\mathbf{Q}^2$. We show only the region of the size $0.1R_0\times0.05R_0$. The symmetry axis is shown by a white line. (c) The numerical grids in the same region as (b).

$R_{ring}/r_c=\exp[(16/\pi)(1/12+K_{24}/K)-1]$, where r_c is the defect core size of the order of the nematic coherence length and K and K_{24} are the Frank elastic constant in the one-constant approximation and the saddle-splay elastic constant,

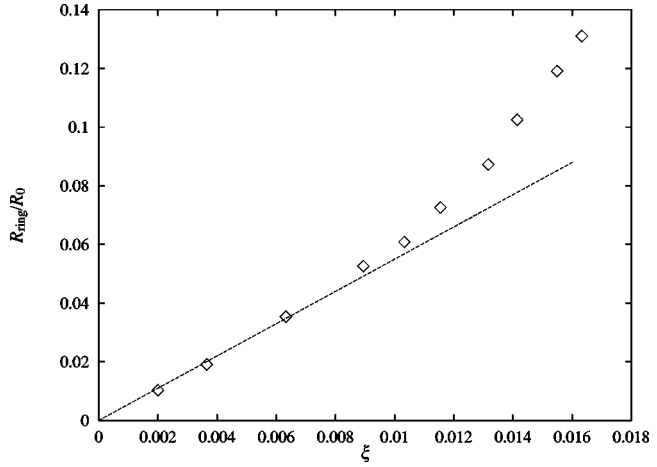

FIG. 2. The radius of the defect ring as a function of ξ. The dashed line represents $R_{ring}/R_0=5.5\xi$.

respectively [23]. They drew a conclusion that $R_{ring}<r_c$ by setting $K_{24}=0$. However, it follows from the Cauchy relationship [24] and recent experiments [25] that K_{24} can be of the order of K. In our simulation the one-constant form of the elastic energy in terms of a tensor order parameter corresponds to taking $K_{24}=K/2$. With this choice of K_{24}, the ring configuration becomes stable because $R_{ring}/r_c\sim7>1$. We also note that the effect of the saddle-splay elasticity to stabilize the hedgehog ring disclination has already been addressed in a qualitative manner by Lavrentovich *et al.* [26] and that the more quantitative analysis based on the treatment of Mori and Nakanishi [27] also yields the same qualitative result [28].

In conclusion, we have investigated numerically the structure of a topological defect in a nematic liquid crystal around a spherical particle with strong homeotropic anchoring on the surface. We have used the technique of adaptive mesh refinement, so that the resolution can be made fine enough to study the situation where the nematic coherence length is of the order $10^{-3}R_0$, with R_0 being the radius of the spherical particle. We have paid attention to the less trivial hedgehog

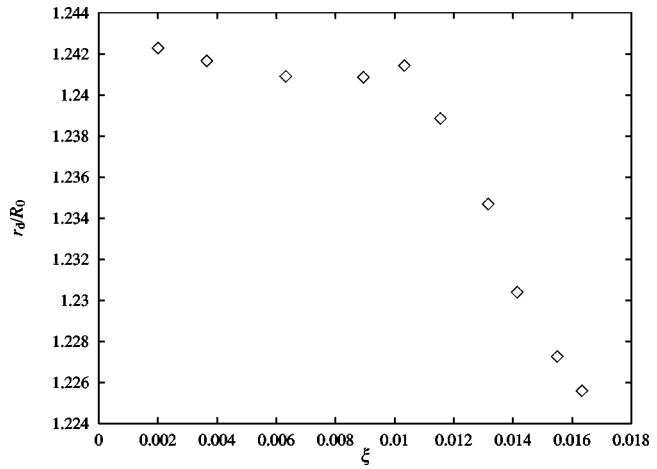

FIG. 3. The distance of the center of the defect ring r_d from the center of the spherical particle as a function of ξ.

configuration and have shown that the hedgehog defect is made up of a small ring rather than a point as argued in the previous experimental and theoretical studies. The ring radius in the hedgehog configuration can be as large as $0.13R_0$, at least in a metastable state. Finally we note that although the maximum radius of the stable defect ring corresponding to the hedgehog configuration is of the order 50 nm when the nematic coherence length is the typical value 10 nm, the nematic coherence length can take a larger value near the nematic-isotropic transition as pointed out in Ref. [10]. In such a situation the observation of the fine defect structure by an optical method might be possible and we encourage experiments to observe fine structures of the topological defects close to particles immersed in a nematic liquid crystal.

We thank Dr. Keiko M. Aoki for helpful and constructive comments.

[1] N.D. Mermin, Rev. Mod. Phys. **51**, 591 (1979).
[2] H.-R. Trebin, Adv. Phys. **31**, 195 (1982).
[3] P.M. Chaikin and T.C. Lubensky, *Principles of Condensed Matter Physics* (Cambridge University Press, Cambridge, 1995).
[4] S. Chandrasekhar, *Liquid Crystals*, 2nd ed. (Cambridge University Press, Cambridge, 1992).
[5] P.G. de Gennes and J. Prost, *The Physics of Liquid Crystals*, 2nd ed. (Oxford University Press, Oxford, 1993).
[6] P. Poulin, H. Stark, T.C. Lubensky, and D.A. Weitz, Science **275**, 1770 (1997).
[7] P. Poulin and D.A. Weitz, Phys. Rev. E **57**, 626 (1998).
[8] O. Mondain-Monval, J.C. Dedieu, T. Gulik-Krzywicki, and P. Poulin, Eur. Phys. J. B **12**, 167 (1999).
[9] Y. Gu and N.L. Abbott, Phys. Rev. Lett. **85**, 4719 (2000).
[10] E.M. Terentjev, Phys. Rev. E **51**, 1330 (1995).
[11] O.V. Kuksenok, R.W. Ruhwandl, S.V. Shiyanovskii, and E.M. Terentjev, Phys. Rev. E **54**, 5198 (1996).
[12] T.C. Lubensky, D. Pettey, N. Currier, and H. Stark, Phys. Rev. E **57**, 610 (1998).
[13] S.V. Shiyanovskii and O.V. Kuksenok, Mol. Cryst. Liq. Cryst. **321**, 45 (1998).
[14] R.W. Ruhwandl and E.M. Terentjev, Phys. Rev. E **56**, 5561 (1997).
[15] H. Stark, Eur. Phys. J. B **10**, 311 (1999).
[16] D. Andrienko, G. Germano, and M.P. Allen, Phys. Rev. E **63**, 041701 (2001).
[17] J.L. Billeter and R.A. Pelcovits, Phys. Rev. E **62**, 711 (2000).
[18] J.T. Oden, T. Strouboulis, and P. Devloo, Comput. Methods Appl. Mech. Eng. **59**, 327 (1986).
[19] J. Fukuda and H. Yokoyama, Eur. Phys. J. E **4**, 389 (2001).
[20] E. Penzenstadler and H.-R. Trebin, J. Phys. (Paris) **50**, 1027 (1989).
[21] P.C. Hohenberg and B.I. Halperin, Rev. Mod. Phys. **49**, 435 (1977).
[22] The easiest way to achieve the variation of ξ is to change the radius of the particle R_0 with fixed material parameters (A, B, C, and L_1), or the nematic coherence length. Although we can change the nematic coherence length by varying the temperature in real systems, it will also lead to the change in the material parameters, which undermines the situation dealt with in our numerical simulations where the relation $C=-B=3A$ is kept.
[23] Here we have employed the definition of K_{24} so that the density of the divergence elastic energy is $-K_{24}\boldsymbol{\nabla}\cdot[\boldsymbol{n}(\boldsymbol{\nabla}\cdot\boldsymbol{n})+\boldsymbol{n}\times(\boldsymbol{\nabla}\times\boldsymbol{n})]$.
[24] J. Nehring and A. Saupe, J. Chem. Phys. **54**, 337 (1971). In the definition of [23], the Cauchy relation reads $K_{24}=(K_{11}+K_{22})/4$.
[25] G.P. Crawford and S. Žumer, Int. J. Mod. Phys. B **9**, 2469 (1995), and the references cited therein.
[26] O.D. Lavrentovich, T. Ishikawa, and E.M. Terentjev, Mol. Cryst. Liq. Cryst. **299**, 301 (1997).
[27] H. Mori and H. Nakanishi, J. Phys. Soc. Jpn. **57**, 1281 (1988).
[28] J. Fukuda and H. Yokoyama (unpublished).